J. Am. Soc. Mass Spectrom. (2011) 22:1214–1223
DOI: 10.1007/s13361-011-0146-4

RESEARCH ARTICLE

Second Order Rate Constants of Donor-Strand Exchange Reveal Individual Amino Acid Residues Important in Determining the Subunit Specificity of Pilus Biogenesis

Aneika C. Leney,[1] Gilles Phan,[2] William Allen,[2] Denis Verger,[2] Gabriel Waksman,[2] Sheena E. Radford,[1] Alison E. Ashcroft[1]

[1]Astbury Centre for Structural Molecular Biology, Institute of Molecular and Cellular Biology, University of Leeds, Leeds, LS2 9JT, UK
[2]Institute of Structural and Molecular Biology, University College London and Birkbeck College, Malet Street, London, WC1E 7HX, UK

Abstract

P pili are hair-like adhesive structures that are assembled on the outer membrane (OM) of uropathogenic *Escherichia coli* by the chaperone-usher pathway. In this pathway, chaperone-subunit complexes are formed in the periplasm and targeted to an OM assembly platform, the usher. Pilus subunits display a large groove caused by a missing β-strand which, in the chaperone-subunit complex, is provided by the chaperone. At the usher, pilus subunits are assembled in a mechanism termed "donor-strand exchange (DSE)" whereby the β-strand provided by the chaperone is exchanged by the incoming subunit's N-terminal extension (Nte). This occurs in a zip-in-zip-out fashion, starting with a defined residue, P5, in the Nte inserting into a defined site in the groove, the P5 pocket. Here, electrospray ionization-mass spectrometry (ESI-MS) has been used to measure DSE rates in vitro. Second order rate constants between the chaperone-subunit complex and a range of Nte peptides substituted at different residues confirmed the importance of the P5 residue of the Nte in determining the rate of DSE. In addition, residues either side of the P5 residue (P5 + 1 and P5 – 1), the side-chains of which are directed away from the subunit groove, also modulate the rates of DSE, most likely by aiding the docking of the Nte into the P5 pocket on the accepting subunit prior to DSE. The ESI-MS approach developed is applicable to the measurement of rates of DSE in pilus biogenesis in general and demonstrates the scope of ESI-MS in determining biomolecular processes in molecular detail.

Key words: Mass spectrometry, Chaperone-usher pathway, P pilus, Donor strand exchange, Second order rate constant

Introduction

Secretion systems are used by a variety of bacteria to transport proteins across their outer membrane. The secretion of virulence factors, such as toxins, and the assembly of adhesive organelles on the bacterial cell surface are

Received: 22 February 2011
Revised: 28 March 2011
Accepted: 1 April 2011
Published online: 10 May 2011

Electronic supplementary material The online version of this article (doi:10.1007/s13361-011-0146-4) contains supplementary material, which is available to authorized users.

Correspondence to: Sheena Radford; *e-mail:* s.e.radford@leeds.ac.uk, Alison Ashcroft; *e-mail:* a.e.ashcroft@leeds.ac.uk

crucial steps in the transmission of infection and, hence, are possible targets for antimicrobial reagents [1]. One type of secretion system, the chaperone-usher pathway, acts to assemble large hair-like structures called pili on the outer membrane of gram negative bacteria [2]. These adhesive pili are essential for pathogenesis and play a major role in urinary tract infections [3].

P pili from uropathogenic *Escherichia coli* are one of the most studied chaperone-usher systems to date [4, 5]. P pili are assembled by the membrane bound PapC usher, and consist of six subunits (PapG, PapF, PapE, PapK, PapA, and PapH), each 2 nm in diameter, arranged in a specific order (Figure 1a) [6]. PapG has an adhesion domain and is the first subunit translocated across the outer membrane. This adhesin binds to host tissues, via a digalactose binding domain, and initiates bacterial infection [7]. Between the adapter subunits, PapF and PapK, is the major component of the flexible tip fibrillum, PapE, which is present in five to 10 copies [8]. After the assembly of the flexible tip, thousands of PapA subunits translocate across the outer membrane and assemble into a rigid right-handed helix [9]. Finally, pilus assembly terminates by incorporating a single copy of PapH [10].

Once translocated across the inner membrane into the periplasm, pilus subunits bind to a chaperone, PapD, to form a stable chaperone-subunit complex [11]. Pilus subunits alone are unstable since they lack the C-terminal β-strand of the canonical immunoglobulin (Ig) fold [12, 13]. However, in the periplasm, PapD donates the seventh β-strand of its first domain (strand G_1) to complete the subunit's Ig fold (Figure 1b), therefore preventing the pilus subunit from degradation by proteases such as DegP [14]. Chaperone-subunit complexes accumulate in the periplasm before being targeted to the usher's N-terminal domain [15, 16], where they undergo a donor-strand exchange (DSE) mechanism in which the chaperone's G_1 strand is gradually replaced by the N-terminal extension (Nte) of an incoming subunit by a "zip-in-zip-out" mechanism whereby the chaperone strand zips out residue by residue, as the incoming Nte zips in (Figure 1c) [17]. On completion of DSE, the usher threads the subunit-subunit complexes through its translocation channel, one at a time, until the entire pilus structure is assembled.

Precisely how thousands of pilus subunits are assembled at the usher rapidly and in a specific order is largely unknown. The differential affinity of chaperone-subunit complexes for the usher's N-terminal domain matches the order in which the subunits are translocated [15]. However, this difference in affinity alone does not explain how the tip subunit, PapG, binds preferentially to the usher over PapA, which is present at a significantly higher concentration than all other pilus subunits combined in the periplasm [18]. It is anticipated, therefore, that a combination of affinity for the usher and differences in DSE rates between subunits play major roles in determining subunit specificity during pilus biogenesis [19].

During DSE, the alternate hydrophobic residues on the Nte of the incoming subunit, termed P1-P5 residues, are inserted into five sites termed P1-P5 pockets in the accepting subunit's groove to form the final subunit-subunit complex (Figure 1b, c). Previous nanoelectrospray mass spectrometry (nanoESI-MS) experiments have been carried out in which different chaperone-subunit complexes were allowed to undergo DSE with all possible subunit Ntes and the apparent rate of DSE was monitored [19]. These experiments showed that the observed rates of DSE between chaperone-subunit:Nte pairs that are found adjacent in the final pilus (termed cognate) are more rapid than chaperone-subunit:Nte pairs that do not undergo DSE in vivo (noncognate). Using experiments in which Nte sequences were swapped between pilus subunits and assembly monitored in vivo, Lee et al. demonstrated that the Ntes of P pili play a predominant role in determining subunit specificity in intact subunits and hence the subunit order in the final pilus [20]. In addition, recent structural and biochemical analysis has revealed that the C-terminal four residues of the Nte play a particularly important role in regulating the rate of DSE, initiating the strand exchange process by insertion of the P5 residue of the Nte into the vacant P5 pocket on the accepting subunit (Figure 1b, c) [10, 19].

In this study, we have used noncovalent ESI-MS to probe further the role of the attacking subunits' Ntes in DSE and, hence, their role in determining subunit specificity. To achieve this, a quantitative nanoESI-MS method has been developed in which the rate of DSE can be measured directly and in real time, without the need for separation of the multi-component reaction mixture prior to analysis. Addition of an internal standard, $PapD_{his}PapH_{Ntd1}$, which is of similar structure but which does not undergo DSE, allowed the protein concentration of the chaperone-subunit complex to be quantified over time, yielding accurate second order rate constants. Using this approach and employing $PapD_{his}PapE_{Ntd}$ as a model system, as this chaperone-subunit complex undergoes the most rapid rate of DSE of all PapDPapX and X_{Nte} peptide pairs, together with a designed range of peptide Ntes containing amino acid substitutions at different sites, we provide data that support the crucial role played by the Ntes' P5 residue in determining the rate of DSE. In addition, we show that residues either side of this residue (i.e., P5 + 1 and P5 − 1) also modulate DSE rates, most likely by positioning the Nte correctly on the accepting subunit prior to DSE. Together, the data provide a quantitative method for the analysis of protein–protein recognition in pilus assembly and reveal new insights into how this specificity is endowed by the sequence of the Nte.

Experimental

Protein Expression and Purification

$PapD_{his}PapE_{Ntd}$ and $PapD_{his}PapH_{Ntd1}$ were expressed periplasmically and purified as described previously [13]. Briefly, plasmids corresponding to $PapD_{his}PapE_{Ntd}$ and $PapD_{his}PapH_{Ntd1}$ were transformed into *Escherichia coli* C600 cells and incubated in Luria-Bertani medium at 37 °C with appropriate antibiotics. At an $O.D._{600}$ of 0.6, protein expression was induced with 1 mM isopropyl β-D-1-

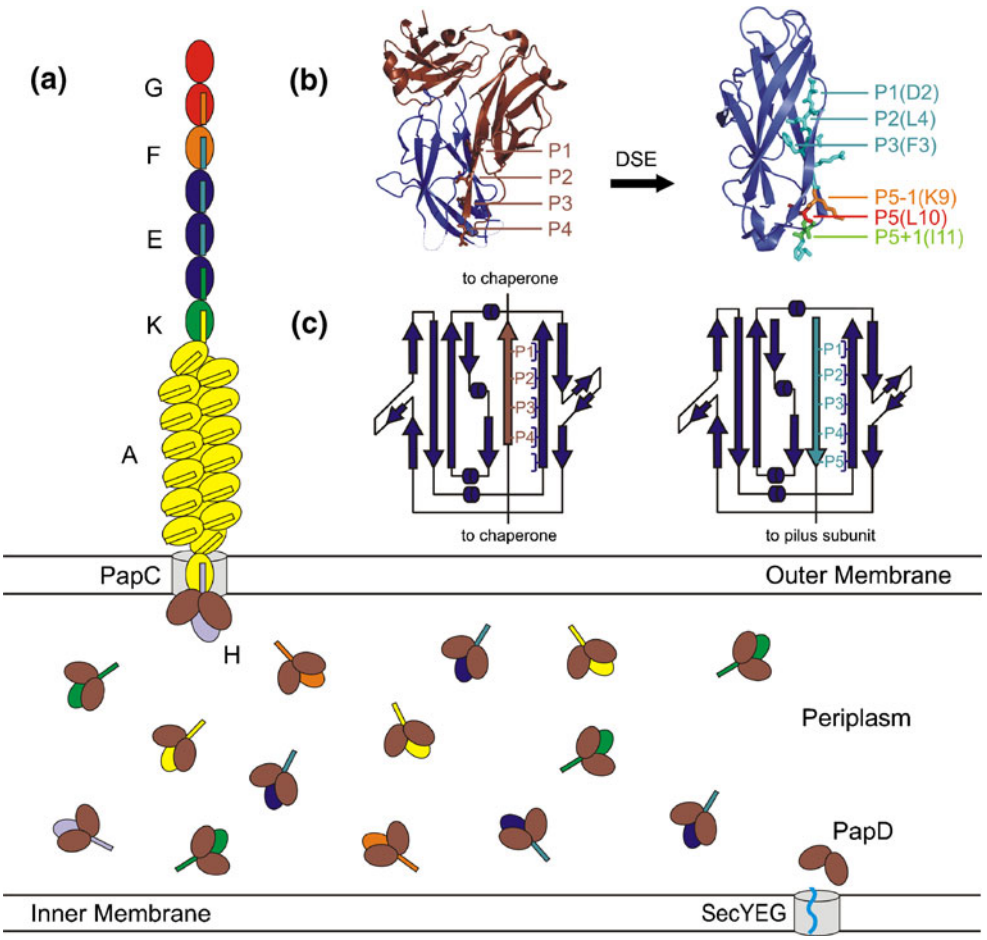

Figure 1. **(a)** Schematic of the chaperone-usher pathway. Pilus subunits translocate across the inner membrane via the Sec machinery and form complexes with the chaperone (PapD; brown) in the periplasm. Chaperone-subunit complexes are targeted to the outer membrane usher (PapC; grey cylinder) where a donor-strand exchange mechanism (DSE) occurs, resulting in the secretion of subunits (G, F, E, K, A, and H; red, orange, blue, green, yellow and purple, respectively) to form the final pilus structure. Each pilus has single copies of subunits G (which has two Ig domains), F, K, and H, five to 10 copies of subunit E, and >1000 copies of subunit A. **(b)** Crystal structure of the chaperone-subunit PapDPapE$_{Ntd}$ (brown-blue) (PDB ID 1N0L) showing residues P1-P4 from the chaperone inserting into the hydrophobic groove of the subunit. The dotted lines represent flexible/unstructured regions. The crystal structure on the right represents the DSE product PapE$_{Ntd}$E$_{Nte}$ (blue-pale blue). The structure was modelled on the PapE$_{Ntd}$K$_{Nte}$ crystal structure (PDB ID 1 N12) with residues from K$_{Nte}$ substituted to the corresponding residues in E$_{Nte}$. The important E$_{Nte}$ residues, P5 – 1 (orange), P5 (red), and P5 + 1 (green) are highlighted. **(c)** Topology diagrams of the chaperone-subunit complex PapDPapE$_{Ntd}$ (brown-blue) and the subunit–Nte complex PapEE$_{Nte}$ (blue-light blue). The chaperone-subunit complex shows the P1-P4 residues on the G$_1$ strand of the chaperone binding to the hydrophobic groove of the subunit completing its Ig fold. The subunit-subunit complex represents the final pilus interaction where the P1-P5 pockets on the subunit are filled by the incoming subunit's N-terminal extension

thiogalactopyranoside (IPTG) and the cells left to grow for a further 3.5 h before harvesting. The cells were lysed using a sucrose/lysozyme method [21]. Both complexes were purified using nickel affinity and hydrophobic interaction chromatographies (HisTrap HP and Phenyl HP; GE Healthcare, Buckinghamshire, UK). PapD$_{his}$PapE$_{Ntd}$ and PapD$_{his}$PapH$_{Ntd1}$ were stored in 20 mM TrisHCl pH 8.0, 150 mM NaCl at −20 °C and dialysed into 5 mM ammonium acetate, pH 6.0 immediately prior to use.

PapE self-polymerizes in vivo, hence a truncated construct, PapE$_{Ntd}$, was used throughout this study in which residues 2–11 of the Nte of PapE (E$_{Nte}$) are deleted [13]. PapD$_{his}$PapH$_{Ntd1}$ is also a truncated construct in which the proline-rich region of the Nte (residues 2–22) is deleted to aid solubility [10]. These constructs have been shown not to self-polymerize and to be suitable models as donor-strand acceptors [13].

N-Terminal Extension Peptides

All peptides were purchased from Bio-synthesis Inc. (Lewisville, TX, USA) and were dissolved in 5 mM ammonium acetate, pH 6.0. To increase solubility, two lysine residues were added to the C-terminus of each Nte sequence (not shown in Figures) and the C-terminus of each peptide was amidated. Previous control experiments comparing the rates of DSE using peptides with and without the additional Lys–Lys sequence confirmed that these residues do not affect the kinetics of DSE [19].

Mass Spectrometry Data Acquisition and Processing

Chaperone-subunit complex $PapD_{his}PapE_{Ntd}$ (25 μM) was incubated at 22 °C with 250 μM N-terminal extension peptide in 5 mM ammonium acetate (pH 6.0). Aliquots (1 μL) were removed at regular time intervals and $PapD_{his}PapH_{Ntd1}$ (5 μM, 9 μL) added immediately before mass spectral acquisition using a LCT Premier mass spectrometer (Micromass UK Ltd., Manchester, UK) equipped with a NanoMate Triversa nanoESI source (Advion Biosciences Inc., Ithaca, NY, USA). Caesium iodide clusters were used as an external calibrant and the following instrumental parameters were set: capillary voltage 1.75 kV, sample cone 70 V, source temperature 50 °C. MassLynx ver. 4.1 software (Micromass UK Ltd., Manchester, UK) was used to process the data. Mass spectra were smoothed twice using the Savitsky-Golay algorithm and centered according to peak area.

Derivation of Second Order Rate Constants

The derived equation for the DSE rate constant was based on the assumption that one chaperone-subunit complex, PapD-PapX, reacts with one Nte of an incoming subunit, X_{Nte}, to form a subunit-Nte complex, PapX-X_{Nte}, via a ternary intermediate, PapDPapX-X_{Nte} (Eq 1).

$$\begin{aligned} \mathrm{PapDPapX} + \mathrm{X_{Nte}} &\underset{k_{-1}}{\overset{k_1}{\rightleftharpoons}} \mathrm{PapDPapX} \\ \mathrm{PapDPapX} - \mathrm{X_{Nte}} &\underset{k_{-2}}{\overset{k_2}{\rightleftharpoons}} \mathrm{PapD} + \mathrm{PapX} - \mathrm{X_{Nte}} \end{aligned} \quad (1)$$

During DSE, chaperone-subunit complexes undergo conformational changes to form subunit-Nte complexes that are thermodynamically extremely stable [22–24]. Thus, it is unlikely that backward DSE reactions occur and k_{-2} can be assumed to be negligible. We were able to characterize a transient chaperone-subunit-Nte intermediate in the Saf pilus system [17], a system related to Pap. However, in Pap, this intermediate does not accumulate during the DSE reaction of P pili and, hence, is not observed in the mass spectra of DSE reactions [19]. Once this complex forms, DSE must therefore occur rapidly for this system suggesting that the binding of the Nte to the chaperone-subunit complex (k_1) is the rate limiting step in the DSE reaction of P pili. Based on these assumptions, Eq 1 can be fitted to a second order rate equation from which the rate constants, k_1 and k_{-1}, can be calculated (Eq 2). For this study, since no DSE intermediate was observed [19] it can be assumed from Eq 1 that $k_2 >> k_{-1}$, and hence k_{-1}[PapDPapX-X_{Nte}] can be approximated to zero (Eq 3).

$$\frac{-\mathrm{d[PapDPapX]}}{\mathrm{dt}} = k_1[\mathrm{PapDPapX}][\mathrm{X_{Nte}}] + k_{-1}[\mathrm{PapDPapX} - \mathrm{X_{Nte}}] \quad (2)$$

$$\frac{-\mathrm{d[PapDPapX]}}{\mathrm{dt}} = k_1[\mathrm{PapDPapX}][\mathrm{X_{Nte}}] \quad (3)$$

The above rate equation (Eq 3) can be integrated and rearranged in terms of chaperone-subunit concentration, [PapDPapX] (Eq 5) based on Eq 4 that states that the decrease in the concentration of the chaperone-subunit complex is equal to the loss of Nte peptide over time, since one chaperone-subunit reacts with one peptide during DSE.

$$[\mathrm{X_{Nte}}]_t = [\mathrm{X_{Nte}}]_0 - \left([\mathrm{PapDPapX}]_0 - [\mathrm{PapDPapX}]_t\right) \quad (4)$$

where $[X_{Nte}]_0$ is the initial concentration and $[X_{Nte}]_t$ is the concentration at time t.

$$[\mathrm{PapDPapX}]_t = y\left\{\frac{[\mathrm{PapDPapX}]_0 e^{-10^{\log k_1}\left([\mathrm{X_{Nte}}]_0 - [\mathrm{PapDPapX}]_0\right)t} - \left(\frac{[\mathrm{PapDPapX}]_0^2 e^{-10^{\log k_1}\left([\mathrm{X_{Nte}}]_0 - [\mathrm{PapDPapX}]_0\right)t}}{[\mathrm{X_{Nte}}]_0}\right)}{1 - \left(\frac{[\mathrm{PapDPapX}]_0 e^{-10^{\log k_1}\left([\mathrm{X_{Nte}}]_0 - [\mathrm{PapDPapX}]_0\right)t}}{[\mathrm{X_{Nte}}]_0}\right)}\right\} \quad (5)$$

where y is the dilution factor with the internal standard, $PapD_{his}PapH_{Ntd1}$, prior to mass spectral acquisition.

Determination of Second Order Rate Constants

To determine the relative concentration of each species during the DSE, nanoESI-MS analyses of the reaction were performed at different times as described above and the areas of the three most abundant $PapD_{his}PapE_{Ntd}$ ions (11+, 12+, and 13+ charge states) were summed and expressed as a fraction of the 12+, 13+, and 14+ charge state ions arising from the $PapD_{his}PapH_{Ntd1}$ internal standard ($PapD_{his}PapH_{Ntd1}$ is known to be unable to undergo DSE [10]). The three most intense charge state ions were chosen for each species as other charge states were lower in intensity and often difficult to distinguish clearly from background ions. Plots of the $PapDPapE_{Ntd}$:$PapD-PapH_{Ntd1}$ ratio against time were fitted to Eq 5 to determine the second order rate constant of DSE. Data are expressed as a percentage of the initial $PapD_{his}PapE_{Ntd}$:$PapD_{his}PapH_{Ntd1}$ ratio before addition of peptide. The parameters from triplicate and duplicate experiments are reported for the P5, P5 – 1, and P5 + 1 substituted E_{Nte} peptides and the substituted chimeric peptides, respectively, along with the standard error between replicates.

Results and Discussion

Second Order Rate Constants of DSE Determined Using NanoESI-MS

To establish the role of individual residues in the Ntes of different peptides in determining the rate of DSE, nano-ESI-MS was used to determine the microscopic rate constants of DSE both quantitatively and in real time. DSE reactions were carried out between the chaperone-subunit complex $PapD_{his}PapE_{Ntd}$ and a designed set of substituted Nte peptides. To determine quantitatively the loss of chaperone-subunit complex, $PapD_{his}PapE_{Ntd}$, as DSE proceeds, an internal standard, $PapD_{his}PapH_{Ntd1}$, was added to the reaction mixture immediately prior to mass spectral analysis. $PapD_{his}PapH_{Ntd1}$ is an ideal, noncovalently bound internal standard since this complex is structurally similar to other PapDPapX complexes but is unable to undergo DSE as its P5 pocket is blocked to allow this subunit to terminate pilus biogenesis [10]. Using this approach, ion intensity was shown to correlate linearly with protein concentration (Figure 2a, b). As a consequence, by measuring the $PapD_{his}PapE_{Ntd}$:$PapD_{his}PapH_{Ntd1}$ ion intensity ratio within each mass spectrum, the concentration of $PapD_{his}PapE_{Ntd}$ can be determined accurately in real time as DSE proceeds, from which the second order rate constant of DSE can be determined using Eq. 5 above.

Mass spectra of the DSE reaction between $PapD_{his}PapE_{Ntd}$ (theoretical mass 40,064 Da) and the E_{Nte} peptide (theoretical mass 1644 Da) are shown in Figure 2c. All reaction components were identified by their unique charge state envelope with a mass accuracy of <0.05% (Supplementary Information, Table S1). On addition of E_{Nte}, the $PapD_{his}PapE_{Ntd}$ ion intensity decreases and the intensity of ions arising from the DSE products $PapD_{his}$ and $PapE_{Ntd}E_{Nte}$ increase. Notably, a control in which no peptide was added confirmed that the loss of $PapD_{his}PapE_{Ntd}$ ion intensity is a result of the DSE reaction with E_{Nte} (Supplementary Information Figure S1). From these data, the ion intensity of $PapD_{his}PapE_{Ntd}$ was determined versus time (Figure 3a) and the data fitted to determine the second order rate constant of DSE of 0.32 $M^{-1}s^{-1}$, in reasonable agreement with the rate of 0.03 $M^{-1}s^{-1}$ reported by others for Fim pilus DSE [25]. The quantitative nanoESI-MS method described thus allows determination of second order rate constants for complex reactions with ease and an accuracy that enables detailed

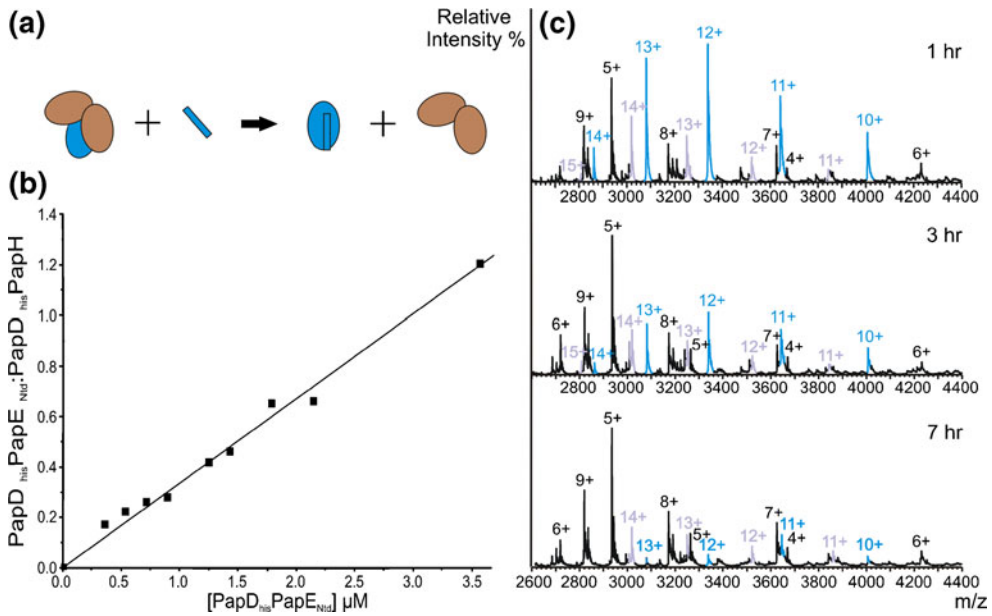

Figure 2. **(a)** Simplified DSE mechanism in which a chaperone-subunit complex (brown-blue, respectively) reacts with an N-terminal extension (Nte) of an incoming subunit (shown as blue bar) resulting in the subunit-Nte product and release of the chaperone. **(b)** Calibration of the relative intensity of $PapD_{his}PapE_{Ntd}$ ions to the internal standard ($PapD_{his}PapH_{Ntd1}$), resulting from increasing the ratio of the $PapD_{his}PapE_{Ntd}$ concentration in the sample. **(c)** NanoESI mass spectra of the DSE reaction between $PapD_{his}PapE_{Ntd}$ and E_{Nte} after 1 h (top), 3 h (middle), and 7 h (bottom). The blue charge state series of ions corresponds to $PapD_{his}PapE_{Ntd}$, and the lilac charge state series of ions to the internal standard, $PapD_{his}PapH_{Ntd1}$. The charge state series of ions corresponding to the DSE products ($PapD_{his}$ and $PapE_{Ntd}$-E_{Nte}) and to $PapE_{Ntd}$ (which appears to be a product of gas phase dissociation from $PapE_{Ntd}$-E_{Nte} as this species is not detected in the starting material and the intensity of these ions can be increased or decreased by judicious use of the ESI sample cone voltage) are shown in black. The rate constant was measured from the decrease in intensity of the 11+, 12+, and 13+ ions originating from $PapD_{his}PapE_{Ntd}$, compared with the 12+, 13+, and 14+ ions of the internal standard

analysis of the role of individual residues in controlling the rate and specificity of pilus assembly.

The P5 Residue in DSE is Important in Determining Subunit Specificity

Previously, by using E_{Nte} and H_{Nte}-derived peptides in which the C-terminal five residues were swapped, we have shown that the C-terminal half of the Nte plays a crucial role in determining DSE rates [19]. Thus, the present study was focused on the P5, P5 + 1, and P5 – 1 residues, since P4 is a glycine in the Ntes of all PapX subunits. We first used the quantitative nanoESI-MS method described above to determine the second order rate constant of DSE in order to quantify the effect of substitutions of the P5 residue in the Nte of PapE. Accordingly, substitutions were made at the P5 residue of a synthetic peptide equivalent to the N-terminal 12 residues of PapE (E_{Nte}), from leucine to either valine or alanine (Figure 3b), and the second order rate constants for DSE with $PapD_{his}PapE_{Ntd}$ were determined using the nanoESI-MS approach described (Table 1). The experiment revealed that the DSE rate constant decreases from 0.32 $M^{-1}s^{-1}$ for the wild type E_{Nte} sequence to 0.10 $M^{-1}s^{-1}$ and 0.09 $M^{-1}s^{-1}$ for the valine and alanine substituted peptides, respectively (Figure 3). The results support the view that the P5 residue of the Nte in the incoming subunit is a critical determinant of the rate of DSE, presumably by modulating the efficiency of the DSE initiation. As a consequence, only minor modifications of the steric fit between the P5 and the P5 pocket result in a significant decrease in the DSE rate constant.

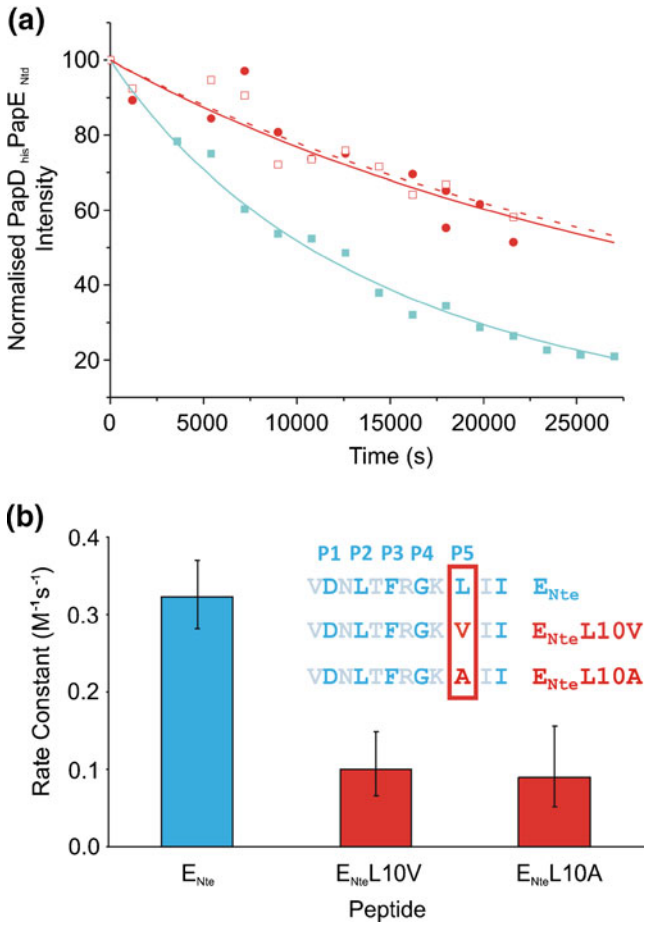

Figure 3. **(a)** The decrease of the normalized $PapD_{his}PapE_{Ntd}$ concentration (determined from the relative ion intensity of $PapD_{his}PapE_{Ntd}$:$PapD_{his}PapH_{Ntd1}$) over time during a DSE reaction with E_{Nte} (blue), and the P5 substituted peptides E_{Nte}L10V (red squares), and E_{Nte}L10A (red circles). **(b)** Second order DSE rate constants for the reaction of the P5 substituted E_{Nte} peptides with $PapD_{his}PapE_{Ntd}$. The average of three second order rate constants (k) is shown for each DSE reaction, together with the standard error between replicates. The insert shows the Nte peptide sequences used in the DSE reactions. Residues that insert into the subunits' hydrophobic groove are highlighted in bold font. Also, the modified P5 residues (L10V and L10A), which insert into the groove, are coloured red

The P5 + 1 and P5 – 1 Residues Modulate DSE

Building on the observation that the P5 residue of the Nte is crucial in determining the rate of DSE, the effect of adjacent residues either side of the P5 residue (termed P5 + 1 and P5 – 1) were next investigated. Although the side-chains of the P5 + 1 and P5 – 1 residues are directed away from the subunit's hydrophobic groove in the crystal structure of the DSE product (Figure 1b) [13], these residues could nonetheless play a role in the progress of the DSE reaction and thus be important determinants of subunit specificity. To investigate the potential role of the P5 – 1 and P5 + 1 residues in determining the rate of DSE, E_{Nte} peptides were designed in which these residues were substituted individually with alanine in the variants E_{Nte}K9A and E_{Nte}I11A, respectively (Figure 4a) and the rate of DSE with $PapD_{his}PapE_{Ntd}$ was determined using these peptides by nanoESI-MS. The resulting second order DSE rate constant decreased from 0.32 $M^{-1}s^{-1}$ for the wild-type E_{Nte} to 0.12 $M^{-1}s^{-1}$ on substitution from isoleucine to alanine at the P5 + 1 position (Figure 4a). Remarkably, this difference in rate constant is similar in magnitude to that of the valine or alanine substitution at the P5 residue, suggesting that the P5 + 1 and the P5 residues are equally important in determining the rate of DSE for this subunit:Nte pair (Table 1). In comparison, substitution at the P5 – 1 position decreased the rate of DSE only slightly (from 0.32 $M^{-1}s^{-1}$ for wild-type to 0.22 $M^{-1}s^{-1}$ for E_{Nte}K9A) (Figure 4a) implying that the P5 – 1 residue has a relatively minor effect in determining the rate of DSE.

As the residues immediately adjacent to the P5 residue in E_{Nte} were found to influence the DSE rate, we next investigated the effect of these residues on DSE in $PapD_{his}PapE_{Ntd}$ by substituting residues from the noncognate H_{Nte} sequence into the sequence of E_{Nte} at the P5 – 1, P5, and P5 + 1 positions (Figure 4b). If residues at the P5 – 1, P5, and P5 + 1 sites are generally important in modulating the rate of DSE, the DSE rate constant with these substituted peptides

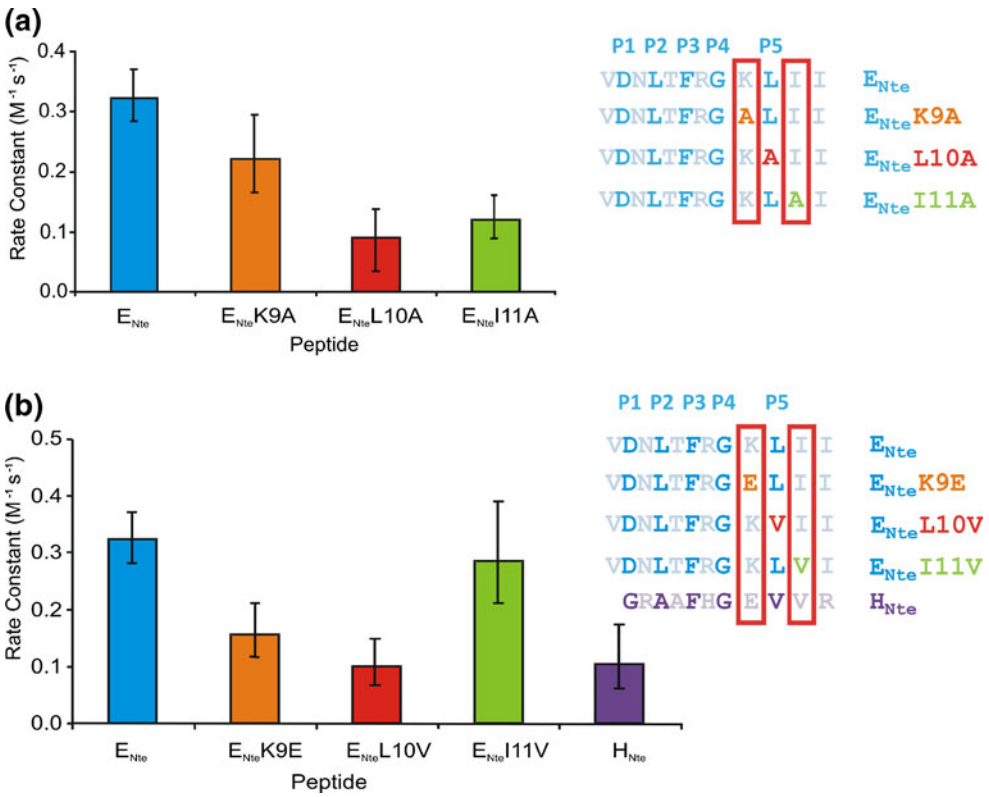

Figure 4. **(a)** Second order DSE rate constants between $PapD_{his}PapE_{Ntd}$ and peptides E_{Nte} (blue), E_{Nte}K9A (orange), E_{Nte}L10A (red), and E_{Nte}I11A (green). The insert shows the Nte peptide sequences used where alanine is substituted individually into E_{Nte} at positions P5 – 1 (K9A), P5 (L10A), and P5 + 1 (I11A). **(b)** Second order DSE rate constants between $PapD_{his}PapE_{Ntd}$ and peptides E_{Nte} (blue), E_{Nte}K9E (orange), E_{Nte}L10V (red), E_{Nte}I11V (green), and H_{Nte} (purple). The insert shows the Nte peptide sequences where H_{Nte} residues are substituted individually into E_{Nte} at positions P5 – 1 (K9E), P5 (L10V), and P5 + 1 (I11V). P1 – P5 residues that insert into the hydrophobic groove of the final subunit are highlighted in bold font

would be expected to decrease substantially, possibly to that of slowest $PapD_{his}PapE_{Ntd}$/Nte DSE reaction, i.e., that with its noncognate peptide (H_{Nte}) [19]. Second order rate constants for the cognate (E_{Nte}) and noncognate (H_{Nte}) Nte with $PapD_{his}PapE_{Ntd}$ are shown for comparison in Figure 4b. Substitution of the P5 residue from leucine (in E_{Nte}) to valine (in H_{Nte}) in the variant E_{Nte} L10V demonstrates that replacement of a critical residue at the DSE initiation site reduces the rate constant of DSE substantially, to a rate equivalent to that observed for the reaction with H_{Nte} (Figure 4b and Table 1). Strikingly, substitution from lysine (the P5 – 1 residue in E_{Nte}) to glutamate (the equivalent residue in H_{Nte}) in the variant E_{Nte} K9E also decreased the second order rate constant substantially, to a rate comparable to that with H_{Nte} (Figure 4b and Table 1). In comparison, substitution of

Table 1. The second order DSE rate constants (pH 6.5, 22 °C) between $PapD_{his}PapE_{Ntd}$ and all substituted peptides used in this study. Rate constants are displayed in terms of both logk and the derived rate constant, k (reported in Figures 3, 4, and 5). The standard errors between triplicate and duplicate DSE reactions are shown for the P5, P5–1, and P5 + 1 substituted E_{Nte} peptides and the substituted chimeric peptides, respectively

Peptide	Residue substituted	Rate constant, logk ($\mu M^{-1}s^{-1}$)	Rate constant, k ($M^{-1}s^{-1}$)
E_{Nte}	None	–6.49±0.06	0.32 (+ 0.05, –0.04)
E_{Nte} L10V	P5	–7.00±0.24	0.10 (+ 0.05, –0.03)
E_{Nte} L10A	P5	–7.05±0.17	0.09 (+ 0.07, –0.04)
E-H_{Nte} V10L	P5	–6.35±0.04	0.45 (+ 0.05, –0.04)
E_{Nte} K9A	P5 – 1	–6.66±0.13	0.22 (+ 0.07, –0.06)
E_{Nte} K9E	P5 – 1	–6.80±0.13	0.16 (+ 0.06, –0.04)
E-H_{Nte} E9K	P5 – 1	–7.44±0.36	0.04 (+ 0.05, –0.02)
E_{Nte} I11V	P5 + 1	–6.54±0.13	0.29 (+ 0.10, –0.08)
E_{Nte} I11A	P5 + 1	–6.92±0.13	0.12 (+ 0.04, –0.03)
E-H_{Nte} V11I	P5 + 1	–7.00±0.15	0.10 (+ 0.04, –0.03)
E-H_{Nte}	None	–7.31±0.19	0.05 (+ 0.03, –0.02)

isoleucine to valine at the P5 + 1 position E_{Nte} I11V had very little effect on the DSE rate constant, with only a minor decrease from 0.32 $M^{-1}s^{-1}$ for E_{Nte} to 0.29 $M^{-1}s^{-1}$ with E_{Nte}I11V (Figure 4b and Table 1).

The above H_{Nte} substituted peptides show differences in the relative importance of the P5 – 1 and P5 + 1 sites compared with those of the alanine scan (Figure 4a), where the P5 + 1 substitution had a greater effect on DSE than the P5 – 1 substitution. The roles of the P5 + 1 and P5 – 1 residues, therefore, are dependent on the precise nature of the side chain introduced. The larger effect of the E_{Nte}K9E substitution compared with the E_{Nte}K9A substitution at the P5 – 1 position (Table 1) suggests that the positive charge is involved in electrostatic interactions that play a role in DSE initiation. Decreasing the size of the amino acid side chain at the P5 + 1 site from isoleucine (in E_{Nte}) to valine (the equivalent residue in H_{Nte}), or further to alanine, decreased the DSE rate constant (Table 1), a trend comparable to that observed at the P5 position (Figure 3). This decrease in side-chain volume may prevent hydrophobic surface interactions taking place which are needed to dock the Nte onto the chaperone-subunit complex before the chaperone's G_1 strand can unzip from the subunit's hydrophobic groove.

P5 + 1 and P5 – 1 Residues Alone Cannot Restore the Fast Kinetics of E_{Nte}

Previous experiments using chimeric peptides in which the N-terminal seven residues of one peptide Nte is fused to the C-terminal five residues of another peptide's Nte demonstrated that the C-terminal region of the Nte alone determines the rate of DSE [19]. To investigate the extent of the P5 + 1 and P5 – 1 residues' roles in determining the rate of DSE further, we next used E-H_{Nte} chimeric peptides which undergo very slow rates of DSE (Figure 4b) [19] and substituted E_{Nte} residues individually at the P5 – 1, P5, or P5 + 1 positions with the aim of increasing the rate of DSE to mirror that obtained between $PapD_{his}PapE_{Ntd}$ and E_{Nte}. A control reaction with peptide E-H_{Nte} confirmed that residues C-terminal to the glycine residue at P4 are important in determining the rate of DSE (Figure 5). Substitution of E_{Nte} residues back into E-H_{Nte} individually at the P5 – 1 and P5 + 1 positions in E-H_{Nte} (i.e.; E-H_{Nte}E9K and E-H_{Nte}V11I, respectively) had little effect on the second order rate constants of DSE (Table 1, Figure 5). However, the E-H_{Nte}V10L substitution, which introduces the cognate P5 leucine residue of E_{Nte} into E-H_{Nte}, increases the DSE rate constant to 0.45 $M^{-1}s^{-1}$, a value similar to that of the cognate reaction rate constant with E_{Nte} (Figure 5). These results demonstrate that in the absence of the P5 residue, the P5 + 1 and P5 – 1 residues cannot restore the DSE rate to that of the cognate reaction. However, if the cognate P5 residue is present in the Nte, the P5 + 1, and P5 – 1 residues act to modulate DSE rates (Figure 4), aiding the docking of the Nte into the empty P5 pocket of the accepting subunit.

Conclusions

An *in vitro* method has been developed to determine second order rate constants of DSE reliably and rapidly using nanoESI-MS. By addition of an internal standard, $PapD_{his}PapH_{Ntd1}$, loss of the substrate, $PapD_{his}PapE_{Ntd}$, can be measured quantitatively in real time from within a complex reaction mixture. This builds on previous ESI-MS methods in which only the apparent rate of DSE was determined [19, 26] by allowing accurate second order rate constants to be determined. In addition, the method developed allows DSE reactions to be monitored over reduced reaction times thus minimising problems associated with solvent evaporation, complex dissociation, and protein precipitation, which inevitably increase with reaction time. The sensitivity of nanoESI-MS, the low volumes of sample required, and the ability to monitor individual, noncovalently bound components within a complex mixture throughout a reaction make this an

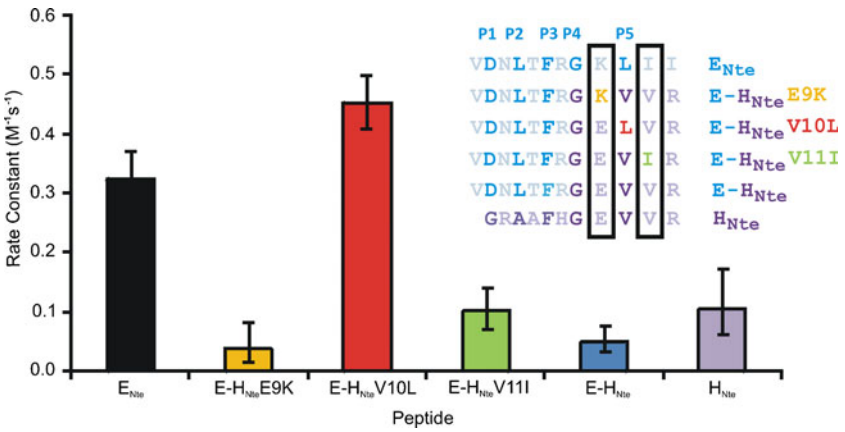

Figure 5. Second order DSE rate constants between $PapD_{his}PapE_{Ntd}$ and peptides E_{Nte} (black), E-H_{Nte}E9K (orange), E-H_{Nte}V10L (red), E-H_{Nte}V11I (green), E-H_{Nte} (blue), and H_{Nte} (purple). The insert shows the Nte peptide sequences used in the DSE reactions. P1 – P5 residues that insert into the final subunit's hydrophobic groove are highlighted in bold font. The substituted P5 – 1, P5, and P5 + 1 residues are coloured in orange, red, and green, respectively

ideal technique for investigating the molecular details of biomolecular assembly processes.

The DSE rates measured in this study reveal new information about the role of individual residues in the Nte in controlling binding of the incoming subunit's Nte to the chaperone-subunit complex and, hence, the rate of DSE initiation. The data show that although the side chains of the P5 + 1 and P5 – 1 residues are orientated away from the binding groove towards the solvent in the final subunit-Nte complex (Figure 1b) [13], they play a distinct role in determining the initial contacts and possibly stabilising the Nte-chaperone-subunit complex. Indeed, crystallography data on Fim subunits from Type 1 pili show that residues surrounding the subunits' hydrophobic groove can flip in and out of the hydrophobic groove on transition from the loose, chaperone-bound state to the more compact subunit-subunit interaction in the pilus tip, thus stabilising the native pilus structure [27]. The results presented here reveal that every residue in the C-terminal half of the Nte is involved in DSE, irrespective of its location in the final DSE product.

The effect of the P5, P5 + 1, and P5 – 1 residues on the rate of DSE demonstrated here, whilst significant, is not sufficient to rationalize the ordering of subunits in the fully assembled pilus, especially once the concentration of different subunits in the periplasm is taken into account (as PapA is found in vast excess to the other subunits). The usher's differential affinities for subunits, along with its catalytic ability, therefore, must also play a key role in controlling the order of subunit polymerization [16, 28]. DSE experiments involving the intact PapC usher will be needed to develop further our understanding of the DSE mechanism, allowing the role of the individual usher domains in defining the rate controlling the order of subunit assembly to be discerned.

Acknowledgments

The authors thank Dr. Bethny Morrissey, University of Leeds, for her help and useful discussions on pilus assembly and mass spectrometry. A.C.L. was funded by a Biotechnology and Biological Sciences Research Council (BBSRC) CASE Ph.D. studentship in collaboration with Micromass UK Ltd.; Manchester, UK (BB/526502/1). The authors acknowledge support for this work by the BBSRC (BB/F012284/1) and the LCT Premier mass spectrometer was funded by the Wellcome Trust (WT 075099/Z/04/Z).

References

1. Cegelski, L., Marshall, G.R., Eldridge, G.R., Hultgren, S.J.: The biology and future prospects of antivirulence therapies. *Nature Rev. Microbiol.* **6**, 17–27 (2008)
2. Thanassi, D.G., Saulino, E.T., Hultgren, S.J.: The chaperone/usher pathway: A major terminal branch of the general secretory pathway. *Curr. Opin. Microbiol.* **1**, 223–231 (1998)
3. Mizunoe, Y., Wai, S.: Bacterial fimbriae in the pathogenesis of urinary tract infection. *J. Infect. Chemother.* **4**, 1–5 (1998)
4. Waksman, G., Hultgren, S.J.: Structural biology of the chaperone-usher pathway of pilus biogenesis. *Nat. Rev. Microbiol.* **7**, 765–774 (2009)
5. Li, H., Thanassi, D.G.: Use of a combined cryo-EM and X-ray crystallography approach to reveal molecular details of bacterial pilus assembly by the chaperone/usher pathway. *Curr. Opin. Microbiol.* **12**, 1–7 (2009)
6. Dhakal, B. K.; Bower, J. M.; Mulvey, M. A.; Moselio, S. Pili, Fimbriae. In: Encyclopedia of Microbiology. Oxford: Academy Press, 2009; pp. 470.
7. Roberts, J.A., Marklund, B.I., Ilver, D., Haslam, D., Kaack, M.B., Baskin, G., Louis, M., Mollby, R., Winberg, J., Normark, S.: The gal (alpha-1-4)gal-specific tip adhesin of *Escherichia coli* P-fimbriae is needed for pyelonephritis to occur in the normal urinary tract. *Proc. Natl. Acad. Sci. U.S.A.* **91**, 11889–11893 (1994)
8. Kuehn, M.J., Heuser, J., Normark, S., Hultgren, S.J.: P pili in uropathogenic *Escherichia coli* are composite fibers with distinct fibrillar adhesive tips. *Nature* **356**, 252–255 (1992)
9. Gong, M.F., Makowski, L.: Helical structure of P pili from *Escherichia coli*—evidence from X-Ray fiber diffraction and scanning-transmission electron-microscopy. *J. Mol. Biol.* **228**, 735–742 (1992)
10. Verger, D., Miller, E., Remaut, H., Waksman, G., Hultgren, S.: Molecular mechanism of P pilus termination in uropathogenic *Escherichia coli*. *EMBO Rep.* **7**, 1228–1232 (2006)
11. Lindberg, F., Tennent, J.M., Hultgren, S.J., Lund, B., Normark, S.: PapD, a periplasmic transport protein in P pilus biogenesis. *J. Bacteriol.* **171**, 6052–6058 (1989)
12. Sauer, F.G., Futterer, K., Pinkner, J.S., Dodson, K.W., Hultgren, S.J., Waksman, G.: Structural basis of chaperone function and pilus biogenesis. *Science* **285**, 1058–1061 (1999)
13. Sauer, F.G., Pinkner, J.S., Waksman, G., Hultgren, S.J.: Chaperone priming of pilus subunits facilitates a topological transition that drives fiber formation. *Cell* **111**, 543–551 (2002)
14. Bakker, D., Vader, C.E.M., Roosendaal, B., Mooi, F.R., Oudega, B., Degraaf, F.K.: Structure and function of periplasmic chaperone-like proteins involved in the biosynthesis of K88 and K99 fimbriae in Enterotoxigenic *Escherichia coli*. *Mol. Microbiol.* **5**, 875–886 (1991)
15. Dodson, K.W., Jacobdubuisson, F., Striker, R.T., Hultgren, S.J.: Outer-membrane PapC molecular usher discriminately recognizes periplasmic chaperone pilus subunit complexes. *Proc. Natl. Acad. Sci. U.S.A.* **90**, 3670–3674 (1993)
16. Ng, T.W., Akman, L., Osisami, M., Thanassi, D.G.: The usher N terminus is the initial targeting site for chaperone-subunit complexes and participates in subsequent pilus biogenesis events. *J. Bacteriol.* **186**, 5321–5331 (2004)
17. Remaut, H., Rose, R.J., Hannan, T.J., Hultgren, S.J., Radford, S.E., Ashcroft, A.E., Waksman, G.: Donor-strand exchange in chaperone-assisted pilus assembly proceeds through a concerted β strand displacement mechanism. *Mol. Cell* **22**, 831–842 (2006)
18. Li, Q.Q., Ng, T.W., Dodson, K.W., So, S.S.K., Bayle, K.M., Pinkner, J.S., Scarlata, S., Hultgren, S.J., Thanassi, D.G.: The differential affinity of the usher for chaperone-subunit complexes is required for assembly of complete pili. *Mol. Microbiol.* **76**, 159–172 (2010)
19. Rose, R.J., Verger, D., Daviter, T., Remaut, H., Paci, E., Waksman, G., Ashcroft, A.E., Radford, S.E.: Unraveling the molecular basis of subunit specificity in P pilus assembly by mass spectrometry. *Proc. Natl. Acad. Sci. U.S.A.* **105**, 12873–12878 (2008)
20. Lee, Y.M., Dodson, K.W., Hultgren, S.J.: Adaptor function of PapF depends on donor strand exchange in P pilus biogenesis of *Escherichia coli*. *J. Bacteriol.* **189**, 5276–5283 (2007)
21. Neu, H.C., Heppel, L.A.: The release of ribonuclease into medium when *Escherichia coli* cells are converted to spheroplasts. *J. Biol. Chem.* **239**, 3893–3900 (1964)
22. Jones, C.H., Pinkner, J.S., Nicholes, A.V., Slonim, L.N., Abraham, S. N., Hultgren, S.J.: FimC is a periplasmic PapD-like chaperone that directs assembly of type-1 pili in bacteria. *Proc. Natl. Acad. Sci. U.S.A.* **90**, 8397–8401 (1993)
23. Zavialvo, A.V., Berglund, J., Pudney, A.F., Fooks, L.J., Ibrahim, T.M., MacIntyre, S., Knight, S.D.: Structure and biogenesis of the capsular F1 antigen from *Yersinia pestis*: Preserved folding energy drives fiber formation. *Cell* **113**, 587–596 (2003)

24. Zavialvo, A.V., Tischenko, V.M., Fooks, L.J., Brandsdal, B.O., Aqvist, J., Zav'yalov, V.P., MacIntyre, S., Knight, S.D.: Resolving the energy paradox of chaperone/usher-mediated fibre assembly. *Biochem. J.* **389**, 685–694 (2005)
25. Vetsch, M., Erilov, D., Molière, N., Nishiyama, M., Ignatov, O., Glockshuber, R.: Mechanism of fibre assembly through the chaperone-usher pathway. *EMBO Rep.* **7**, 734–738 (2006)
26. Verger, D., Rose, R.J., Paci, E., Costakes, G., Daviter, T., Hultgren, S., Remaut, H., Ashcroft, A.E., Radford, S.E., Waksman, G.: Structural determinants of polymerization reactivity of the P pilus adaptor subunit PapF. *Structure* **16**, 1724–1731 (2008)
27. Le Trong, I., Aprikian, P., Kidd, B.A., Thomas, W.E., Sokurenko, E. V., Stenkamp, R.E.: Donor strand exchange and conformational changes during *E. coli* fimbrial formation. *J. Struct. Biol.* **172**, 380–388 (2010)
28. Nishiyama, M., Ishikawa, T., Rechsteiner, H., Glockshuber, R.: Reconstitution of pilus assembly reveals a bacterial outer membrane catalyst. *Science* **320**, 376–379 (2008)